Electrocatalysis of organics for electrolysis and/or fuel cells: Some thoughts on using the ratio of forward to backward peak current as a measure of electrocatalyst efficiency and/or poisoning

Yaovi Holade, Teko Napporn, Kouakou Boniface Kokoh

Electrocatalysis of organics for electrolysis and/or fuel cells: Some thoughts on using the ratio of forward to backward peak current as a measure of electrocatalyst efficiency and/or poisoning

Yaovi Holade,[1,2,3] Teko W. Napporn[2,4] and Kouakou Boniface Kokoh[2,4*]

[1]Institut Européen des Membranes, IEM, UMR 5635, Univ Montpellier, ENSCM, CNRS, 34090 Montpellier, France

[2]French Research Network on Hydrogen (FRH2), Research Federation No. 2044 CNRS, BP 32229, Nantes CEDEX 3 44322, France

[3]Institut Universitaire de France (IUF), 75005 Paris, France

[4]Université de Poitiers, IC2MP UMRCNRS 7285, 86073 Poitiers, France

Corresponding author: Kouakou Boniface, Kokoh (boniface.kokoh@univ-poitiers.fr)

Abstract

In the current context of sustainability, the selective electrocatalytic transformation of biomass-derived organic substances into value-added products should offer vast design possibilities for power generation or the electrosynthesis of fuels and commodity chemicals. In this contribution, we have examined a number of concepts concerning the electrocatalysis of organic molecules for which noble metals cannot be excluded from the electrocatalyst composition without compromising the significant energy savings promised in electrolyzers (up to 50% for H_2 co-production compared to conventional water electrolysis). The widespread practice of using the ratio of forward peak current to backward peak current as a measure of activity, anti-poison capacity or removal of adsorbed poisons or intermediates is unsuitable based voltammetry and spectroelectrochemical analysis.

Keywords

electrocatalysis, electrosynthesis, electroconversion, biomass, biofuels, bio-based chemicals, cyclic voltammetry, spectroelectrochemistry, ion exchange membrane.

Introduction

Historically, alongside organic electrosynthesis [1,2], the study of the catalytic electrooxidation of organic compounds such as methanol, ethanol, formic acid, glycerol and oligosaccharides, was driven by demand for fuel cells (FCs), since these liquid fuels offer a handling advantage over H_2, which is still more than 90% derived from fossil fuels [3-6]. The growth over the last five years is exponentially greater, because in addition to hydrogen evolution reaction (HER), an efficient anode is critical for other energy-intensive cathodic reactions such as CO_2 reduction reaction (CO2RR) and N_2 reduction reaction (N2RR) for the electrosynthesis of value-added compounds in electrolysis cells (ECs) [7-13]. In fact, the kinetics of OER being at least an order of magnitude slower than HER, substituting OER with organic compounds having thermodynamically lower oxidation potentials than water activation should enable up to 50% electricity savings compared to traditional water electrolysis [7-9,14-16]. For ECs, achieving high selectivity in the oxidation of organics at consequent current densities (0.2-2 A cm^{-2}) [17] and moderate cell voltage is challenging when noble metals (Pt, Au, Pd, etc.) are excluded from the electrocatalyst composition. For organic-fueled FCs (ethanol, glycerol, etc.), anode electrocatalysts based on the so-called "abundant and cheaper" metals (M = Ni, Ag, Fe, Mn, etc.) have not yet guarantee lower anode's potential than that of the cathode (oxygen reduction reaction, ORR), generally operating between 0.8 and 1.0 V vs RHE (reversible hydrogen electrode). Hence, for both ECs and FCs purpose, a compromise in terms of the anode's potential, selectivity, and current density can be provided by low noble metal(s) loading electrocatalysts, which may include, in addition to abundant metals, either Pt for its dehydrogenating properties at low potential, Au for improved stability and/or selectivity, or Pd which behaves as an intermediate between Pt and Au.

Since a number of reviews have extensively dealt with the advantages and disadvantages of many organic electrochemical reactions [1,2,16,18,19], it seems redundant to us to repeat these arguments yet again. So, in this contribution, we concentrate on certain aspects of fundamental understanding of organic molecules' electrocatalysis. We discuss the interesting open question of whether the ratio of forward peak current to backward peak current, I_f/I_b, can be used as a metric for the efficiency/poisoning of electrocatalysts, a widespread practice [20-25].

Organics electrooxidation paired to HER, NRR, CO2RR, etc.

Before tackling the question of peak current ratios, we first discuss the scope regarding the electrooxidation of organics. Figure 1a suggests that the electrooxidation of organics (glycerol, glucose, etc.) should lower the cell voltage and thus improve the energy efficiency of electrolysis, since the relationship between the required electricity and the cell voltage is W[kWh/kg(H_2)] = 26.59×U_{cell}[V] [14,15], wherein $U_{\text{cell}} = E_{(\text{anode})} - E_{(\text{cathode})}$. Therefore, $E_{(\text{anode})}$ should ideally be low; this is a challenge for noble-metal-free electrode materials which so far catalyze the oxidation of organic compounds at potentials above 1 V vs RHE. For high electrode potential of 1.4-1.7 V vs RHE [26-28], the carbon-carbon bond rupture is frequent, in addition the competition with OER, hence a small gain in energy efficiency at industrial level current densities of 0.2-2 A cm^{-2}. Under acidic media, CO_2 can be the final product of the organics electrooxidation, provided that it is sent back to cathode [7,8,10,19], however, the situation is complicated in alkaline media where the carbonation and/or precipitation is detrimental to the electrolyzer performance [29,30].

Since the electrooxidation of an organic molecule is a proton-coupled electron transfer process (PCET, influenced by the p*K*a of the organic molecule [31]), the kinetics may be slower than that of OER. For example, while the theoretical oxidation potential of 5-hydroxymethyl-furfural (HMF) to 2,5-furandicarboxylic acid (FDCA) is about 0.3 V vs RHE [32], lower than the potential for OER (1.23 V vs RHE), an electrode potential of 1.3-1.6 V vs RHE was necessary to 0.36 A cm^{-2} at Cr-Ni$(OH)_2$/nickel foam electrocatalysts (faradaic efficiency of 90-98% [27,28]). Different characterization has revealed that the needed concomitant reduction of Ni(III) to Ni(II) as the electron acceptor to promote the HMF dehydrogenation occurs within the MOOH (M = Co-Fe-Mo-Cr) region of 1.3-1.5 V vs RHE [27,28,33]. This indirect electrooxidation is driven by the active redox center MOOH/M$(OH)_2$ [34]. The electrochemical performance can be augmented by transition metals phosphides or sulfides where the electron density transfer from partially and positively charged metal centers $M^{\delta+}$ (M = Ni, Co, etc.) to partially and negatively charged $X^{\delta-}$ (X = P, S) promote the dehydrogenation [28,35]. The three fundamental driving forces being the long-range geometric lattice deformation, the synergy (multiple metals), and the short-range electronic charge transfer effects [36]. Furthermore, the governing mechanism for electrode materials comprising noble metals (direct electrooxidation sites) and non-noble metals (indirect electrooxidation sites) remains unraveled when the anode potential is above 1.2-1.4 V vs RHE, where MOOH/M$(OH)_2$ electrochemistry predominates.

To consider the above applications, we question in the following a common practice of basing the catalytic activity of electrode materials on the I_f/I_b ratio.

Can I_f/I_b be used as a measure of efficiency/poisoning of electrocatalysts?

Typically, the cyclic voltammogram (CV) of Pt in an electrolyte in the presence of methanol, formic acid, glycerol, etc., shows at least one peak during the forward scan and the same during the backward scan. We note that Pt, Pd and Au are metals for which a straightforward discriminating observation is possible (Figure 1b for Pd [20]). On Ni, for example, the behavior [33] is similar to bioelectrocatalysts [37-39], i.e. there is no clear presence of a peak during the backward scan. It has been claimed that [20-25], an increase of I_f/I_b indicates: (i) that the electrooxidation performance of the intermediates is enhanced (Figure 1c) as well as a better anti-poisoning ability [20,22], (ii) a superior electrocatalytic activity [21]. Some reports attributed the forward scan peak to organics electrooxidation and the backward scan peak to the removal of carbonaceous species generated in the forward scan [23]. Another explanation would be that the reduction of metal oxides during the backward scan liberates the surface that was oxidized during the forward scan, allowing the electrooxidation of new reactant molecules, thus producing an oxidation peak [3,40,41]. The two underlying questions are then, as there is a (main) peak during the anodic scan (forward) and a peak during the cathodic scan (backward) for the CV of electrooxidation of organics on a metallic electrocatalyst (for instance Pt, Au, Pd): (i) What exactly is electrooxidized during the backward scan? (ii) Can I_f/I_b be used as a metric of efficiency and/or does I_f/I_b formally assess the poisoning tolerance of electrocatalysts? To answer these questions, a careful analysis of the electrochemical signature is necessary (Figures 2a-d & 3a) together with spectroelectrochemistry (Figure 3b-d) put forward by the authors of the present paper.

A comparative analysis of CVs in the absence and presence of the reactive organic molecule provides the first tentative answers, Figure 2a (Au) and Figure 2b (Pt) for the electrooxidation of formic acid [3]. Firstly, the peak during the anodic scan in the presence of the substrate begins to decrease when reaching the region of metal oxide formation. Secondly, the onset of the cathodic scan peak in the presence of the substrate coincides with the start of the reduction of metal oxides to metal in the absence of the substrate. So, intuitively, the simplest explanation would be to postulate that the new voltammetric wave during cathodic scanning results from the electrooxidation of new substrate molecules on the freshly released active sites. This

hypothesis seems logical, given that the CV joins the blank one at low potential range. We note that the *I*(E) response to an excitation *E*(t) being the sum of all current contributions, an oxidation current does not mean that there is no concomitant reduction. The CV profile on bio-electrocatalysts (Figure 3a) does not show any significant difference because the nature of the active sites does not change like PGMs-based electrodes. So, one can conclude that the origin of the cathodic scan peak depends on the kinetics of the metal oxides reduction, which is in agreement with similar observations during the ORR [42,43].

The CV and first-principles density functional theory (DFT) results in Figure 2c-d show that the cathodic direction starts in the region where the electrocatalyst surface is covered by PdO species, which *d*-band center (ε_d, relative to the Fermi level) is shifted away from the Fermi level compared to $Pd(OH)_x$ and Pd surfaces [42]. This results into lower activity according to Nørskov theory [44], the closer the position of ε_d toward the Fermi level, the stronger the interactions with adsorbates. So, the kinetics of noble metal-based oxides reduction, the surface coverage with hydroxyl species as well as the concentration of the reactant might be the driving force behind the second wave of oxidation during the backward scan. Assuming that the theory of "strongly adsorbed poisons" is true, and reasoning by the absurd, we have hypothesized that [41], using spectroelectrochemistry in single potential alteration infrared reflectance spectroscopy (SPAIRS, CV coupled to FTIRS), the bands characteristic of the oxidation products of the anodic scan will be absent when doing the opposite (Figure 3b). For the forward scan from 0.05 to 1.40 V vs RHE (Figure 3c), the increase in current is accompanied by the synchronous appearance of IR bands (upwards for reactant consumption and downwards for product formation, mainly gluconate, detailed assignment in ref. [41]). Now, going from 1.40 to 0.05 V vs RHE (Figure 3d) to unequivocally determine the nature of the process that marks the return peak, we can see that the SPAIRS shows the appearance of the same bands. The increase in band intensity is therefore indicative of increasing gluconate production, in phase with the increase in current. These results therefore invalidate the widespread explanation that the backward peak (Figure 2b) is essentially due to the oxidation of "poisons formed during the forward (strongly adsorbed intermediates)". Conclusively, the origin of the peak observed in the reverse voltammetric wave during the oxidation of an organic molecule on a noble metal-based electrocatalyst is not only the result of the oxidation of "possible poisons formed during the forward scan" but also the oxidation of substrate molecules on the active sites released by the reduction of metal oxides and the elimination of other organic intermediates.

It is worth pointing out that using fast-scan CVs (except in molecular electrochemistry to mitigate irreversibility situations) to probe the organics oxidation kinetics should be used with caution and not straightforwardly to conclude on steady-state faradaic processes because of the significant capacitive response. Potential, catalyst, electrolyte, coverage, etc. dictate the steps of PCET, i.e. the nature of the bond that breaks first [28,45-50]. Whereas this knowledge is essential to guide the design of efficient electrode materials, existing studies are divergent, some proposing that the organic molecule approaches the catalytic surface via the OH group [28,45-47] while others [48,49] suggest that among C-H, O-H and C-C bonds, the C-H bond is the easiest to break. For gold, we have shown that the increased population of hydroxylated species at high potentials favors C-H dehydrogenation while the metallic surface favors O-H dehydrogenation at lower potentials together resulting in an oxide-like gold surface [50].

Conclusions and outlook

In this contribution, we have reviewed some of the basic concepts of electrocatalysis of organic molecules on a metal surface, which have been controversially explained. The presence of an intense oxidation peak during the backward scan of electrooxidation of an organic compound on noble metal-based electrocatalysts is being considered a guarantee of efficiency (anti-poisoning, superior electrocatalytic activity, removal of carbonaceous species generated in the forward scan), in contrast to the seminal models. It can be concluded that the backward peak (negative scanning of the electrode potential) results from the electrooxidation of substrate molecules on the active sites released by the reduction of metal oxides and possible adsorbed organic intermediates. Consequently, the ratio of forward peak current to backward peak current (I_f/I_b) should not be always used to gauge the efficiency/poisoning of electrocatalysts as it widespread practiced. Finally, the open question of the first electron transferred, that is, which of the C-H, O-H and C-C bonds breaks first, is still debated and synergetic theory-experiment studies could provide more realistic models.

Declaration of competing interest

The authors declare that they have no known competing financial interests or personal relationships that could have appeared to influence the work reported in this paper.

Data availability

Data will be made available on request.

Acknowledgements

This work received funding from French National Research Agency (ANR-22-CE43-0004, ANR-10-LABX-05-01 LabEx CheMISyst), European Union (ERDF), “Région Nouvelle-Aquitaine”, and “Grand Angoulême”. This work pertains to the French government program “Investissements d’Avenir” (EUR INTREE, reference ANR-18-EURE-0010). Prof. K.B. Kokoh is grateful to the “Fondation Poitiers Université” and EDF for their financial support (R-2024-37) within his green chemistry projects.

References

Papers of particular interest, published within the period of review, have been highlighted as:

* of special interest

** of outstanding interest

1. Hilt G: **Recent advances in paired electrolysis and their application in organic electrosynthesis**. *Curr Opin Electrochim* 2024, **43**:101425. https://doi.org/10.1016/j.coelec.2023.101425.
2. Liu H, Li W: **Recent advances in paired electrolysis of biomass-derived compounds toward cogeneration of value-added chemicals and fuels**. *Curr Opin Electrochim* 2021, **30**:100795. https://doi.org/10.1016/j.coelec.2021.100795.
3. ** Beden B, Çetin I, Kahyaoglu A, Takky D, Lamy C: **Electrocatalytic oxidation of saturated oxygenated compounds on gold electrodes**. *J Catal* 1987, **104**:37-46. http://dx.doi.org/10.1016/0021-9517(87)90334-4.

This seminal work on the electrocatalysis of organic molecule postulates that the “adsorbed oxygen atoms” (metal oxides at high potentials) act as inhibitors for the organic oxidation.

During backward sweep, as soon as these metal oxides are reduced, the electrode surface regains its catalytic properties to oxidize new reactant molecules.

4. Biegler T, Koch DFA: **Adsorption and oxidation of methanol on a platinum electrode**. *J Electrochem Soc* 1967, **114**:904. https://dx.doi.org/10.1149/1.2426775.
5. Kokoh KB, Léger JM, Beden B, Huser H, Lamy C: **"On line" chromatographic analysis of the products resulting from the electrocatalytic oxidation of d-glucose on pure and adatoms modified Pt and Au electrodes—Part II. Alkaline medium**. *Electrochim Acta* 1992, **37**:1909-1918. https://doi.org/10.1016/0013-4686(92)87102-6.
6. Caravaca A, Garcia-Lorefice WE, Gil S, de Lucas-Consuegra A, Vernoux P: **Towards a sustainable technology for H_2 production: Direct lignin electrolysis in a continuous-flow polymer electrolyte membrane reactor**. *Electrochem Commun* 2019, **100**:43-47. https://doi.org/10.1016/j.elecom.2019.01.016.
7. Houache MSE, Safari R, Nwabara UO, Rafaïdeen T, Botton GA, Kenis PJA, Baranton S, Coutanceau C, Baranova EA: **Selective electrooxidation of glycerol to formic acid over carbon supported $Ni_{1-x}M_x$ (M = Bi, Pd, and Au) nanocatalysts and coelectrolysis of CO_2**. *ACS Appl Energy Mater* 2020, **3**:8725–8738. https://doi.org/10.1021/acsaem.0c01282.
8. Verma S, Lu S, Kenis PJA: **Co-electrolysis of CO_2 and glycerol as a pathway to**
** **carbon chemicals with improved technoeconomics due to low electricity consumption**. *Nat Energy* 2019, **4**:466-474. https://doi.org/10.1038/s41560-019-0374-6.

This work demonstrates one of the first reliable proof-of-concept of pairing CO2RR with different anode scenarios (OER, glycerol oxidation and glucose oxidation) in an anion exchange membrane-based electrolysis cell. The study also integrates techno-economic aspects. Glycerol as an anode substrate, which achieves a high current density compared with glucose (for the same range of voltage), can reduce electricity consumption by up to 53% compared with OER.

9. Liu W-J, Xu Z, Zhao D, Pan X-Q, Li H-C, Hu X, Fan Z-Y, Wang W-K, Zhao G-H, Jin S, et al.: **Efficient electrochemical production of glucaric acid and H_2 via glucose electrolysis**. *Nat Commun* 2020, **11**:265. https://doi.org/10.1038/s41467-019-14157-3.
10. Luna PD, Hahn C, Higgins D, Jaffer SA, Jaramillo TF, Sargent EH: **What would it take for renewably powered electrosynthesis to displace petrochemical processes?** *Science* 2019, **364**:eaav3506. https://doi.org/10.1126/science.aav3506.
11. Zhou H, Ren Y, Yao B, Li Z, Xu M, Ma L, Kong X, Zheng L, Shao M, Duan H: **Scalable electrosynthesis of commodity chemicals from biomass by suppressing non-**

Faradaic transformations. *Nat Commun* 2023, **14**:5621. https://doi.org/10.1038/s41467-023-41497-y.

12. Wang T, Tao L, Zhu X, Chen C, Chen W, Du S, Zhou Y, Zhou B, Wang D, Xie C, et al.: **Combined anodic and cathodic hydrogen production from aldehyde oxidation and hydrogen evolution reaction**. *Nat Catal* 2022, **5**:66-73. https://doi.org/10.1038/s41929-021-00721-y.
13. Tatin A, Comminges C, Kokoh B, Costentin C, Robert M, Savéant J-M: **Efficient electrolyzer for CO_2 splitting in neutral water using earth-abundant materials**. *Proc Natl Acad Sci* 2016, **113**:5526-5529. https://doi.org/10.1073/pnas.1604628113.
14. Guenot B, Cretin M, Lamy C: **Electrochemical reforming of dimethoxymethane in a proton exchange membrane electrolysis cell: A way to generate clean hydrogen for low temperature fuel cells**. *Int J Hydrogen Energy* 2017, **42**:28128-28139. https://doi.org/10.1016/j.ijhydene.2017.09.028.
15. Holade Y, Tuleushova N, Tingry S, Servat K, Napporn TW, Guesmi H, Cornu D, Kokoh KB: **Recent advances in the electrooxidation of biomass-based organic molecules for energy, chemicals and hydrogen production**. *Catal Sci Technol* 2020, **10**:3071-3112. http://dx.doi.org/10.1039/C9CY02446H.
16. Braun M, Santana CS, Garcia AC, Andronescu C: **From waste to value – Glycerol electrooxidation for energy conversion and chemical production**. *Curr Opin Green Sustainable Chem* 2023, **41**:100829. https://doi.org/10.1016/j.cogsc.2023.100829.
17. Chatenet M, Pollet BG, Dekel DR, Dionigi F, Deseure J, Millet P, Braatz RD, Bazant MZ, Eikerling M, Staffell I: **Water electrolysis: from textbook knowledge to the latest scientific strategies and industrial developments**. *Chem Soc Rev* 2022, **51**:4583-4762. https://doi.org/10.1039/D0CS01079K.
18. Coutanceau C, Neha N, Rafaïdeen T: **Electrocatalytic transformation of biosourced organic molecules**. *Curr Opin Electrochim* 2023, **38**:101210. https://doi.org/10.1016/j.coelec.2023.101210.
19. Tao L, Choksi TS, Liu W, Pérez-Ramírez J: **Challenges and opportunities in synthesizing high volume chemicals from CO_2 without direct H_2 input**. *ChemSusChem* 2020, **13**:6066-6089. https://doi.org/10.1002/cssc.202001604.
20. Ji L, Che H, Qian N, Li J, Luo S, Li X, Wu X, Xu Q, Gong X, Cui X, et al.: **Unconventional s-p-d hybridization in modulating frontier orbitals of carbonaceous radicals on PdBi nanosheets for efficient ethanol electrooxidation**. *Appl Catal B: Env* 2023, **328**:122521. https://doi.org/10.1016/j.apcatb.2023.122521.

21. Chen T, Xu S, Zhao T, Zhou X, Hu J, Xu X, Liang C, Liu M, Ding W: **Accelerating ethanol complete electrooxidation via introducing ethylene as the precursor for the C−C bond splitting**. *Angew Chem Int Ed* 2023, **62**:e202308057. https://doi.org/10.1002/anie.202308057.

22. Sun B, Zhong W, Ai X, Zhang C, Li F-M, Chen Y: **Engineering low-coordination atoms on RhPt bimetallene for 12-electron ethanol electrooxidation**. *Energy Environ Sci* 2024, **17**:2219-2227. http://dx.doi.org/10.1039/D3EE04023B.

23. Li S, Lai J, Luque R, Xu G: **Designed multimetallic Pd nanosponges with enhanced electrocatalytic activity for ethylene glycol and glycerol oxidation**. *Energy Environ Sci* 2016, **9**:3097-3102. http://dx.doi.org/10.1039/C6EE02229D.

24. Qi Z, Xiao C, Liu C, Goh TW, Zhou L, Maligal-Ganesh R, Pei Y, Li X, Curtiss LA, Huang W: **Sub-4 nm PtZn intermetallic nanoparticles for enhanced mass and specific activities in catalytic electrooxidation reaction**. *J Am Chem Soc* 2017, **139**:4762-4768. https://doi.org/10.1021/jacs.6b12780.

25. Liu W, Herrmann A-K, Geiger D, Borchardt L, Simon F, Kaskel S, Gaponik N, Eychmüller A: **High-performance electrocatalysis on palladium aerogels**. *Angew Chem Int Ed* 2012, **51**:5743-5747. http://dx.doi.org/10.1002/anie.201108575.

26. Miao J, Teng X, Zhang R, Guo P, Chen Y, Zhou X, Wang H, Sun X, Zhang L: **"Carbohydrate-Universal" electrolyzer for energy-saving hydrogen production with Co3FePx@NF as bifunctional electrocatalysts**. *Appl Catal B: Env* 2020, **263**:118109. https://doi.org/10.1016/j.apcatb.2019.118109.

27. Yang Z, Zhang B, Yan C, Xue Z, Mu T: **The pivot to achieve high current density for biomass electrooxidation: Accelerating the reduction of Ni^{3+} to Ni^{2+}**. *Appl Catal B: Env* 2023, **330**:122590. https://doi.org/10.1016/j.apcatb.2023.122590.

28. Yang Z, Wang S, Wei C, Chen L, Xue Z, Mu T: **Proton transfer mediator for boosting the current density of biomass electrooxidation to the ampere level**. *Energy Environ Sci* 2024, **17**:1603-1611. http://dx.doi.org/10.1039/D3EE04543A.

29. Rabinowitz JA, Kanan MW: **The future of low-temperature carbon dioxide electrolysis depends on solving one basic problem**. *Nat Commun* 2020, **11**:5231. https://doi.org/10.1038/s41467-020-19135-8.

30. Seger B, Robert M, Jiao F: **Best practices for electrochemical reduction of carbon dioxide**. *Nat Sustain* 2023, **6**:236-238. https://doi.org/10.1038/s41893-022-01034-z.

31. Koper MTM: **Theory of multiple proton-electron transfer reactions and its implications for electrocatalysis**. *Chem Sci* 2013, **4**:2710-2723. http://dx.doi.org/10.1039/C3SC50205H.
32. Yang Y, Mu T: **Electrochemical oxidation of biomass derived 5-hydroxymethylfurfural (HMF): pathway, mechanism, catalysts and coupling reactions**. *Green Chem* 2021, **23**:4228-4254. https://doi.org/10.1039/D1GC00914A.
33. Houache MSE, Cossar E, Ntais S, Baranova EA: **Electrochemical modification of nickel surfaces for efficient glycerol electrooxidation**. *J Power Sources* 2018, **375**:310-319. https://doi.org/10.1016/j.jpowsour.2017.08.089.
34. Fleischmann M, Korinek K, Pletcher D: **The kinetics and mechanism of the oxidation of amines and alcohols at oxide-covered nickel, silver, copper, and cobalt electrodes.** *J Chem Soc, Perkin Trans 2* 1972, **10**:1396-1403. http://dx.doi.org/10.1039/P29720001396.
35. Wang C, Jiang J, Ding T, Chen G, Xu W, Yang Q: **Monodisperse ternary NiCoP nanostructures as a bifunctional electrocatalyst for both hydrogen and oxygen evolution reactions with excellent performance.** *Adv Mater Interfaces* 2016, **3**:1500454. https://doi.org/10.1002/admi.201500454.
36. Strasser P, Koh S, Anniyev T, Greeley J, More K, Yu C, Liu Z, Kaya S, Nordlund D, Ogasawara H, et al.: **Lattice-strain control of the activity in dealloyed core–shell fuel cell catalysts**. *Nat Chem* 2010, **2**:454-460. http://dx.doi.org/10.1038/nchem.623.
37. Milton RD, Wu F, Lim K, Abdellaoui S, Hickey DP, Minteer SD: **Promiscuous glucose oxidase: Electrical energy conversion of multiple polysaccharides spanning starch and dairy milk**. *ACS Catal* 2015, **5**:7218-7225. http://dx.doi.org/10.1021/acscatal.5b01777.
38. Riklin A, Katz E, Willner I, Stocker A, Buckmann AF: **Improving enzyme-electrode contacts by redox modification of cofactors**. *Nature* 1995, **376**:672-675. http://dx.doi.org/10.1038/376672a0.
39. Holade Y, Yuan M, Milton RD, Hickey DP, Sugawara A, Peterbauer CK, Haltrich D, Minteer SD: **Rational combination of promiscuous enzymes yields a versatile enzymatic fuel cell with improved coulombic efficiency**. *J Electrochem Soc* 2017, **164**:H3073-H3082. https://doi.org/10.1149/2.0111703jes.
40. Faverge T, Gilles B, Bonnefont A, Maillard F, Coutanceau C, Chatenet M: **In situ**

** **investigation of D-glucose oxidation into value-added products on Au, Pt, and Pd under alkaline conditions: A comparative study**. *ACS Catal* 2023, **13**:2657-2669. https://doi.org/10.1021/acscatal.2c05871.

This work compares the CV of Au, Pt and Pd bulk electrodes in the NaOH electrolyte in the absence and presence of glucose, gluconic acid and sorbitol. The formation of surface metal oxides (MO_x, M = Au, Pt, Pd) considerably reduces the oxidation current corresponding to organic substances. During the cathodic scan (backward scan), the reduction of these oxidized surface MO_x into metallic surface leads to the reactivation of the surface, resulting in an oxidation peak that is dependent on a number of parameters, such as scan rate, MO_x reduction rate, and surface coverage by adsorbates formed at high potentials.

41. Holade Y, Engel AB, Servat K, Napporn TW, Morais C, Tingry S, Cornu D, Kokoh
** KB: **Electrocatalytic and electroanalytic investigation of carbohydrates oxidation on gold-based nanocatalysts in alkaline and neutral pHs**. *J Electrochem Soc* 2018, **165**:H425-H436. https://doi.org/10.1149/2.0311809jes.

This work leverages spectroelectrochemistry to demonstrate for the first time that the oxidation peak during the reverse sweep (also known as the backward sweep or cathodic sweep) corresponds to the electrooxidation of fresh reagent molecules on freshly released metalloid active sites, following the concomitant reduction of metal oxides formed at high potential

42. Wang Q, Guesmi H, Tingry S, Cornu D, Holade Y, Minteer SD: **Unveiling the pitfalls
* of comparing oxygen reduction reaction kinetic data for Pd-based electrocatalysts without the experimental conditions of the current–potential Curves**. *ACS Energy Lett* 2022, **7**:952-957. https://doi.org/10.1021/acsenergylett.2c00181.

This work establishes that, owing to the difference in the surface state of Pd as a function of potential between 0.3 and 1 V vs RHE, the non-disclosure (possibly unintentional) when recording the polarization curves of ORR is very problematic. The anodic scanning (low to high potentials) leads to a kinetic current density that is 4-15 times larger than the cathodic scanning (high to low potentials).

43. Shinozaki K, Zack JW, Richards RM, Pivovar BS, Kocha SS: **Oxygen reduction reaction measurements on platinum electrocatalysts utilizing rotating disk electrode technique: I. Impact of impurities, measurement protocols and applied corrections**. *J Electrochem Soc* 2015, **162**:F1144-F1158. https://doi.org/10.1149/2.0551512jes.

44. Jeff Greeley, Jens K. Nørskov, Mavrikakis M: **Electronic structure and catalysis on metal surfaces**. *Annu Rev Phys Chem* 2002, **53**:319-348. https://doi.org/10.1146/annurev.physchem.53.100301.131630.

45. Wei L, Sheng T, Ye J-Y, Lu B-A, Tian N, Zhou Z-Y, Zhao X-S, Sun S-G: **Seeds and potentials mediated synthesis of high-index faceted gold nanocrystals with enhanced electrocatalytic activities**. *Langmuir* 2017, **33**:6991-6998. http://dx.doi.org/10.1021/acs.langmuir.7b00964.

46. Ishimoto T, Kazuno H, Kishida T, Koyama M: **Theoretical study on oxidation reaction mechanism on Au catalyst in direct alkaline fuel cell**. *Solid State Ionics* 2014, **262**:328-331. https://doi.org/10.1016/j.ssi.2013.10.020.

47. Caglar A, Düzenli D, Onal I, Tezsevin I, Sahin O, Kivrak H: **A comparative experimental and density functional study of glucose adsorption and electrooxidation on the Au-graphene and Pt-graphene electrodes**. *Int J Hydrogen Energy* 2020, **45**:490-500. https://doi.org/10.1016/j.ijhydene.2019.10.163.

48. * Liu B, Greeley J: **Decomposition pathways of glycerol via C–H, O–H, and C–C bond scission on Pt(111): A density functional theory study**. *J Phys Chem C* 2011, **115**:19702-19709. http://dx.doi.org/10.1021/jp202923w.

This work leverages the first-principles density functional theory (DFT) to interrogate the decomposition of glycerol on Pt(111) via the comparative scission of C–H, O–H and C–C bonds. The dehydrogenation via activation of the C–H bond is thermochemically favored, followed by the O–H bond. Both dehydrogenation transition state energies (C–H and O–H) are much lower than the corresponding transition state energy for C–C bond cleavage.

49. ** Garcia AC, Kolb MJ, van Nierop y Sanchez C, Vos J, Birdja YY, Kwon Y, Tremiliosi-Filho G, Koper MTM: **Strong impact of platinum surface structure on primary and secondary alcohol oxidation during electro-oxidation of glycerol**. *ACS Catal* 2016, **6**:4491-4500. http://dx.doi.org/10.1021/acscatal.6b00709.

This work shows that for the first dehydrogenation step of glycerol oxidation on Pt(111) and Pt(100) single crystal electrodes, carbon-bonded intermediates resulting from the removal of hydrogens bonded to carbon atoms (C–H bond cleavage) are always significantly more stable than oxygen-bonded intermediates resulting from O–H bond cleavage. The energy difference is about 0.2 eV for the Pt(100) electrode and at least 0.5 eV for the Pt(111) electrode.

50. Holade Y, Guesmi H, Filhol J-S, Wang Q, Pham T, Rabah J, Maisonhaute E, Bonniol

** V, Servat K, Tingry S, et al.: **Deciphering the electrocatalytic reactivity of glucose anomers at bare gold electrocatalysts for biomass-fueled electrosynthesis**. *ACS Catal* 2022, **12**:12563-12571. https://doi.org/10.1021/acscatal.2c03399.

This work suggests that in the absence of hydroxyl functions on the gold surface (acid and neutral pH, low electrode potentials), glucose is adsorbed by deprotonation of the O–H group bound to the anomeric carbon (α-anomer) after the first proton-coupled electron transfer (PCET). This produces a more stable oxidized-like gold surface intermediate than the carbon-bonded intermediate resulting from the dehydrogenating PCET of hydrogen directly bonded to the anomeric carbon (C–H bond cleavage, β-anomer).

Figure 1. (**a**) Illustrative half-cell polarization curves of different electrosynthesis scenarios pairing a process at the negative electrode (cathode, (–)) with one at the positive electrode (anode, (+)).. (**b**) CVs recorded at 50 mV s^{-1} in Ar-saturated 0.5 M KOH + 1 M ethanol (room temperature); Reprinted and adapted from Ref. [20], Copyrights 2023, Elsevier B.V. (**c**) Trend in the ratio of the forward peak current density (I_f) to the backward peak current density (I_b), I_f/I_b (or j_f/j_b), from CVs recorded at 50 mV s^{-1} for different electrocatalysts in N_2-saturated 1 M KOH + 1 M ethanol; Reprinted and adapted from Ref. [22], Copyrights 2024, The Royal Society of Chemistry.

Figure 2. (**a**) CVs of bulk Au in 0.5 M H_2SO_4 (80 °C, 20 mV s^{-1}) in the absence (solid lines) and presence of 10 mM HCOOH (dotted lines) and (**b**) CVs of bulk Pt in 0.5 M H_2SO_4 (80 °C, 20 mV s^{-1}) in the absence (solid lines) and presence of 10 mM HCOOH (dotted lines); Reprinted and adapted from Ref. [3], Copyright 1987, Elsevier Inc. (**c**) Impact of the anodic/cathodic direction on the CVs recorded at the disk and ring of a RRDE in the absence and in the presence of O_2 (1 M KOH, 1600 rpm, 10 mV s^{-1}). (**d**) First-principles Density Functional Theory (DFT) calculated local densities of states (LDOSs) of the Pd 4d bands in the three modeled systems (insets of (**c**)): (A) pristine Pd(111), (B) hydroxylated Pd(111), and (C) oxidized Pd(111); Reprinted and adapted from Ref. [40], Copyright 2022, American Chemical Society.

Figure 3. (**a**) CVs at 10 mV s^{-1} of bioelectrode (broader substrate glucose oxidase, bGOx; red dashed line is the control bioelectrode without the redox mediator) in citrate/phosphate buffer (pH 6.5, 0.2 M) in the absence (dashed lines) and in the presence of 100 mM of glucose (solid lines); Reprinted and adapted from Ref. [35], Copyright 2022, American Chemical Society. (**b-d**) Spectroelectrochemistry experiments (0.1 M NaOH, 50 mM glucose, Temperature: 22 ± 2 °C) on $Au_{80}Pt_{20}$/C nano-electrocatalyst: (**b**) CV at 1 mV s^{-1}, (**c**) SPAIRS in the anodic direction and plotted every 0.1 V (except 0.05 and 0.1 V vs RHE) for an initial electrode potential of 0.05 V vs RHE, and (**d**) SPAIRS in the cathodic direction and plotted every 0.1 V (except 0.05 and 0.1 V vs RHE) for an initial electrode potential of 1.40 V vs RHE; Reprinted and adapted from Ref. [39] under a CC BY-NC-ND 4.0 license, Copyright 2018, The Author(s), Published by ECS.

Figure 1

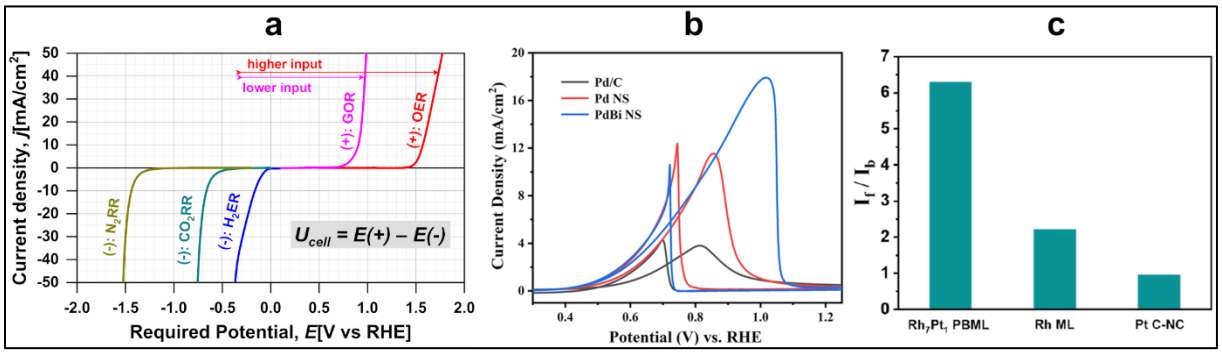
a
b
c
higher input
lower input
(+): GOR
(+): OER
(-): N2RR
(-): CO2RR
(-): H2ER
Ucell = E(+) – E(-)
Current density, j[mA/cm2]
Required Potential, E[V vs RHE]
Pd/C
Pd NS
PdBi NS
Current Density (mA/cm2)
Potential (V) vs. RHE
If / Ib
Rh7Pt1 PBML
Rh ML
Pt C-NC

Figure 2

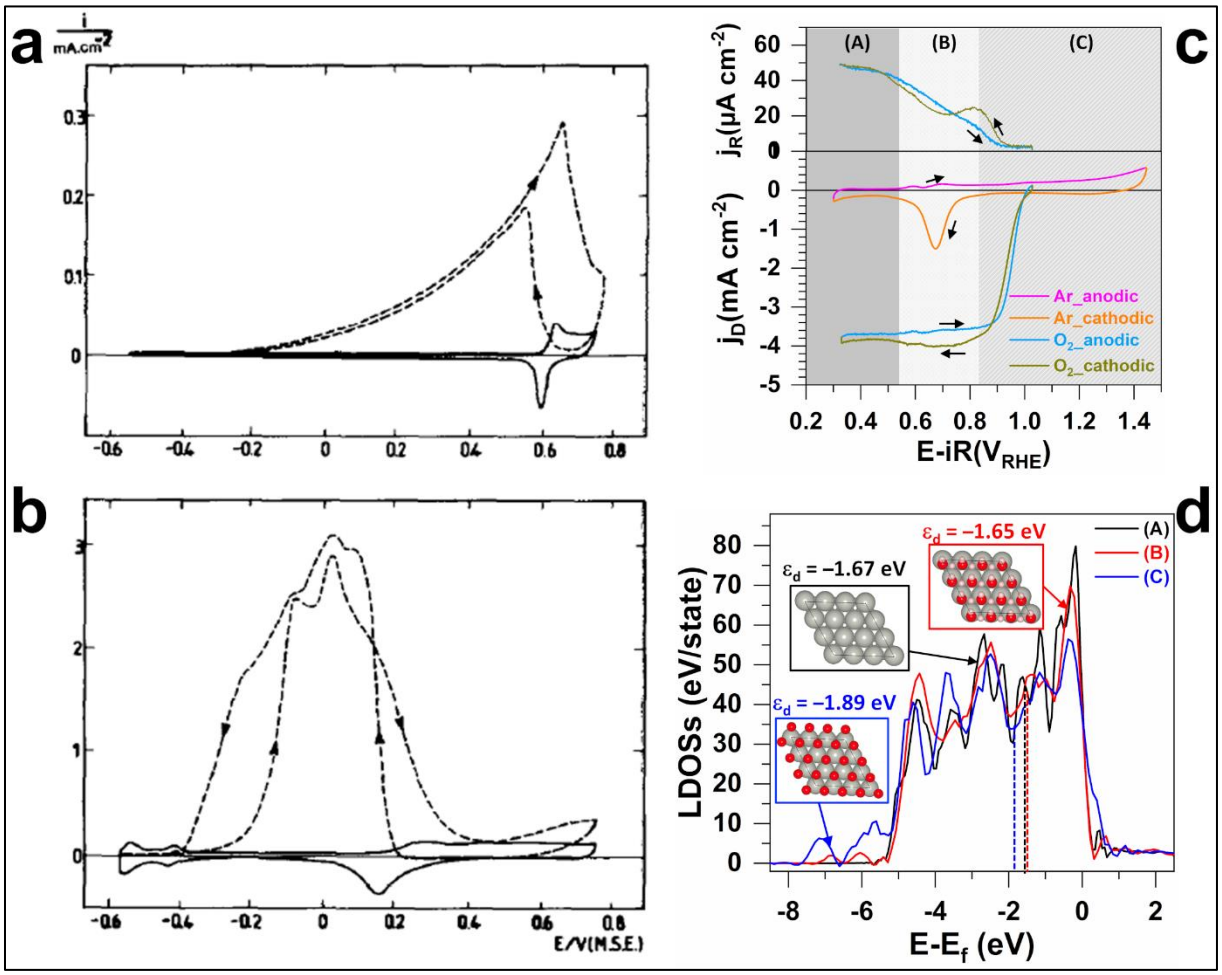
a
i
mA.cm⁻²
b
E/V(M.S.E.)
c
(A)
(B)
(C)
j_R(μA cm^{-2})
j_D(mA cm^{-2})
Ar_anodic
Ar_cathodic
O_2_anodic
O_2_cathodic
E-iR(V_{RHE})
d
ε_d = −1.65 eV
ε_d = −1.67 eV
ε_d = −1.89 eV
LDOSs (eV/state)
E-E_f (eV)

Figure 3

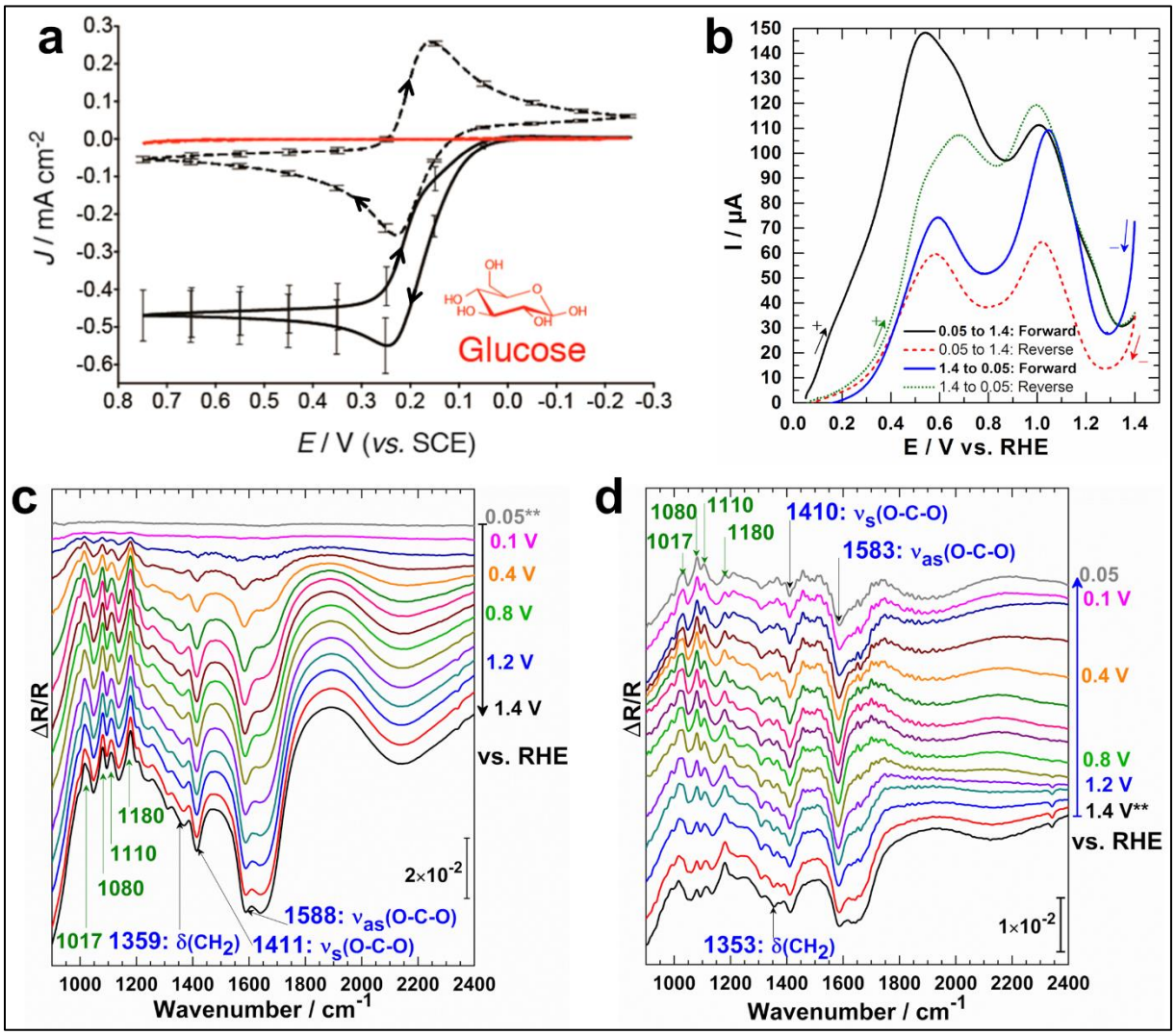
a
J / mA cm-2
E / V (vs. SCE)
Glucose
b
I / µA
E / V vs. RHE
0.05 to 1.4: Forward
0.05 to 1.4: Reverse
1.4 to 0.05: Forward
1.4 to 0.05: Reverse
c
ΔR/R
0.05**
0.1 V
0.4 V
0.8 V
1.2 V
1.4 V
vs. RHE
1180
1110
1080
1017
1359: δ(CH2)
1411: νs(O-C-O)
1588: νas(O-C-O)
2×10-2
Wavenumber / cm-1
d
1080
1110
1017
1180
1410: νs(O-C-O)
1583: νas(O-C-O)
0.05
0.1 V
0.4 V
0.8 V
1.2 V
1.4 V**
vs. RHE
1353: δ(CH2)
1×10-2
Wavenumber / cm-1